SCANNING PROBE MICROSCOPY
AS A COMPREHENSIVE MICROANALYTICAL INSTRUMENTARY

[1,2]O.V. SERGEEV, [1]N.V. GAPONENKO, [1]N.G. LAZAREVA,
[2,3]R.M. CRAMER, [2]R. HEIDERHOFF, [1]V.E. BORISENKO, [2]L.J. BALK

[1] *Belarusian State University of Informatics and Radioelectronics, Minsk, Belarus*

[2] *Bergische Universität Wuppertal, Wuppertal, Germany*

[3] *ALTIS Semiconductor, Paris, France*

This review briefly presents some results of collaborative work on new methods of microanalysis and nanolithography based on scanning probe microscopy and obtained during long-term cooperation between Center of Nanoelectronics and Novel Materials of Belarusian State University of Informatics (Belarus) and Radioelectronics and Bergische Universität Wuppertal (Germany).

Keywords: microscopy, optoelectronics, sol-gel structures.

Preface

Plenty of joint educational and scientific activities were established and successfully realized during for more than twelve years of intensive cooperation between Belarusian State University of Informatics (Belarus) and Radioelectronics and Bergische Universität Wuppertal (Germany).

The bright illustration of particularly fruitful development can be the evolution of the idea to build collaborative work in the field of material research and microanalysis proposed by scientific supervisor of Center of Nanoelectronics and Novel Materials, professor V.E. Borisenko (BSUIR) and professor L.J. Balk, the head of the Department of Electronics (BUW) in 1997. By that time research groups leaded by these scientists were already internationally recognized experts in the areas of nanoelectronics, ULSI technology, Si-based optoelectronics and scanning probe and scanning electron microscopy techniques of microanalysis, correspondingly. The idea to combine wide experience in synthesis of novel low dimensional materials and exceptional potentialities of original analytical methods was attractive and high promising in respect to obtain information never known before or non-confirmed by practice. The joint work had different forms of long terms cooperation like students exchange and personal training, specialized programs of research. As well, some work supported by BUW was done by the joint team with the use of unique facilities of National University of Singapore in 1999. Results on fabrication and characterization of novel low-dimensional materials are widely shown in scientific press and represented at international conferences. This review briefly presents already completed and currently performing joint investigations.

Characterization of Light-Emitting Sol-Gel Structures with Atomic Force Microscopy

Thin films doped with lanthanides attract much attention as prospective bases for integrated optoelectronic devices in photonic technology such as optical waveguides, amplifiers and laser sources

due to their bright and spectral clear luminescence. Sol-gel fabrication of SiO_2, TiO_2, Fe_2O_3, In_2O_3, Al_2O_3 thin films containing optically active trivalent ions of Er, Eu and Tb has been developed and used in BSUIR. In comparison to standard methods like ion implantation, electrochemical doping, pulse laser deposition, molecular beam epitaxy, spark processing and others sol-gel technique shows many important advantages: relatively low cost, simplicity of fabrication, easy chemical content control and regulation, absence of thermal or radiation influence, wide range of substrates that could be used. The matter of our particular interest was the idea to increase efficiency and stability of such films using regular pore surface of anodic alumina as a skeleton ground for them. By consequent spinning, drying and annealing one-, five- and ten-layered erbium-containing titania xerogels were fabricated in the pores of anodic alumina (the pores were about 40 nm in diameter and 70 nm apart, for details see [1]) and on n-type and p-type Si wafers.

Noteworthily, that all films fabricated on anodic alumina substrates show bright photoluminescence even at room temperature of trivalent erbium at 1.53 μm (main telecommunication window) while even 5-layered film on flat Si substrates are not luminescent at all. Moreover, PL intensity increases with the number of xerogel layers (Fig. 1) and the emission from the sample coated ten times is about one order of magnitude greater than for the sample coated in one step. The deposition of ten layers results in about two-fold narrowing of the full width at half maximum (FWHM) of the main erbium related band at 1.53μm (~14 nm) in comparison with the samples coated with five layers (~30 nm). According to the secondary-ion mass spectrometry data sol penetrates throughout the pores to the bottom and distribution of elements is quite uniform along the whole depth. The films are enriched with oxygen (62 at.%) and the common concentration ratio of other components stays almost constant within the depth of porous Al_2O_3, the presence of carbon in the films is less than 1 at.%.
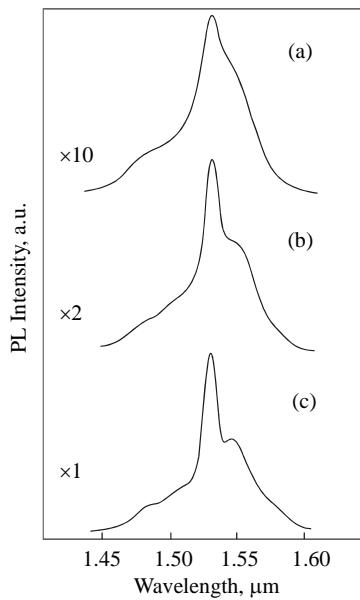

Fig. 1. Room temperature PL spectra at 1.53 μm of erbium doped titania xerogel deposited onto alumina one (a), five (b) and ten (c) times

These facts testify to an improvement of optical activation conditions of the erbium impurity. We could assume as well complete infill of the pore layer with xerogel and formation of flat xerogel film above. Unfortunately SIMS is a point analyzing method and gives no information on surface properties. It would be of a great interest to explore the surface topography of the specimens and to define possible correlation to its luminescent behavior. Traditionally used electron microscopy is not suitable in this case due to the need of additional metallization. The atomic force microscopy for 3-D surface imaging gave us a good chance to confirm with incredibly high resolution the microglobular structure of fabricated films (Fig. 2). It is clearly seen the average size of globules is about 100 nm for five depositions and approximately 200 nm for ten-layered film. Obviously, deposition of new layers leads to growth of xerogel particles that demonstrates continuation of polymerization and polyconden-

86

sation reactions between different layers. After ten depositions the xerogel network is denser and more perfect – surface roughness is less than 50 nm only. Such flat and uniform morphology confirms other results that the pores are filled out completely. The absence of macrocracks and destructions usual for the xerogel films such of thickness formed on non-porous substrates is obvious as well that provided by reliable porous skeleton of anodic alumina.
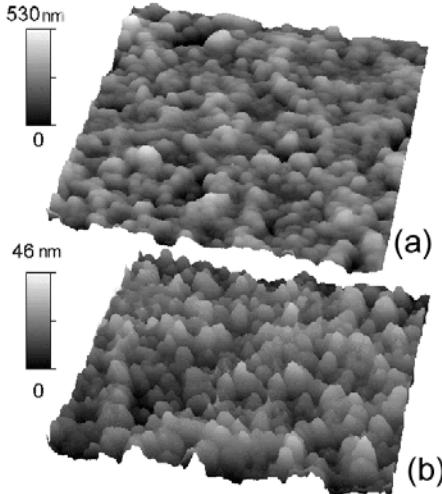

Fig. 2. Topography of five- and ten-layered spin-on titania xerogels on porous anodic alumina

The observed optical properties and high surface quality of erbium-doped titania xerogel on porous alumina make the fabricated structures prospective for optics and optoelectronics.

Scanning Probe Microscopy for Cathodoluminescent Analysis in the Optical Near-Field

Cathodoluminescence (CL) is widely used as non-contact and relatively non-destructive testing of electrical and optical properties of wide gap semiconductors and dielectrics while low energetic photoluminescence method is not so efficient. However, CL spatial resolution is limited by e-beam diameter, energy dissipation in the specimen volume and by drift of minor charge carriers. Practically it is not better than several μm thus it becomes poorly suitable for analysis of novel low dimensional structures and devices. To overcome this limitations the scanning near-field optical microscope (SNOM) has been implemented into the chamber of scanning electron microscope (SEM) that gave a chance to simultaneously depict the surface of specimen and excite CL by e-beam impact with SEM means, explore the surface topography and image the distribution of CL intensity over the surface with incredibly high spatial resolution by the SNOM tapered optical fiber probe (Fig.3, 4) [2].

The possibilities of such hybrid system were demonstrated by investigating yellow surface-emitting GaAsP light emitting diodes (LEDs) where the light output degradation plays a very important role. There are several factors, such as crystal defects, contamination etc., which can cause degradation in the light output signal. Therefore, a comprehensive recognition of these defects and their subsequent characterization has to be carried out. This analysis has to be done at a nanoscopic level to ensure that even smallest structures with modified properties can be evaluated. The SE and the CL image of the investigated LED detected at primary electron energies of 15 keV are shown on the upper part of Fig. 5. As can be seen, the luminescence is homogeneous over the whole device. Only a few defects are detectable within the GaAsP. The degradation mechanism can be clarified by high spatial resolution analyses. NF-CL investigations were performed on the same device and the results are illustrated at the foot of Fig. 5. Topography effects that are superimposed on the NF-CL can be explained by the theory of evanescent light. This contrast is not detectable with conventional CL. In addition, submicron specimen surface defects are observable due to these near-field conditions.
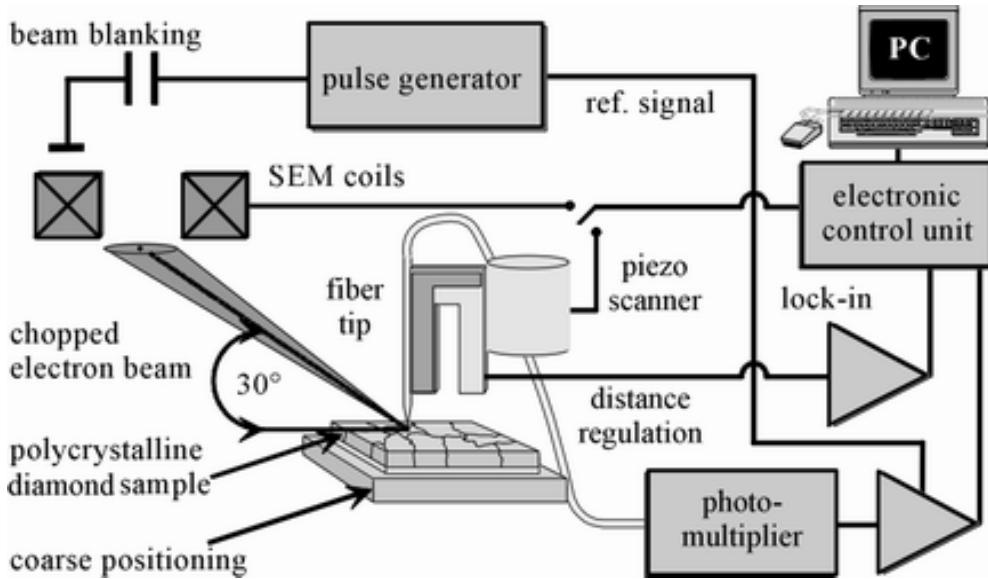
Fig. 3. Scanning electron microscope / scanning near-field optical microscope hybrid system
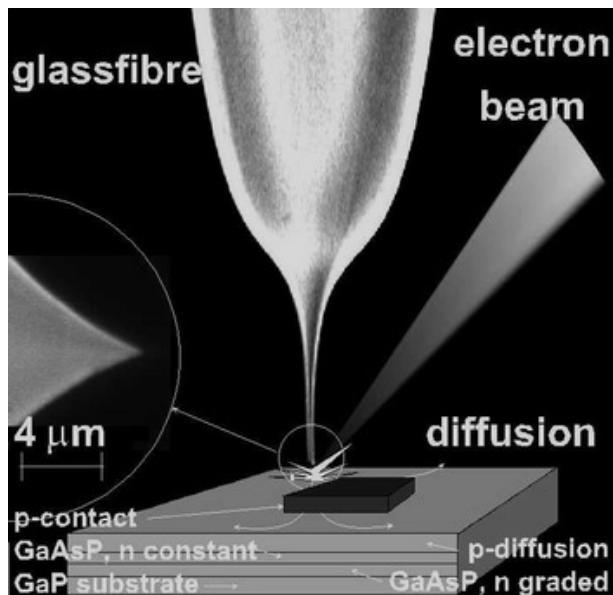

Fig. 4. The view "probe over the sample". Separation distance is few nm only

Near-Field Cathodoluminescence from Nanoscopic Diamond

Cathodoluminescence from diamond is studied for more than 50 years. It is established in the characterization of natural, high-pressure synthesized, and CVD diamond. More than 100 of the optical centers that have been documented for diamond give rise to luminescence. A lot of efforts were made to recognize and characterize even smallest defects in diamond. TEM superimposed with CL need an intensive destructive sample preparation to achieve a high spatial resolution. To ensure that even smallest structures with modified material properties can be evaluated we performed near-field detection cathodoluminescence (NF-CL) analyses on MWCVD diamond in a scanning near-field optical microscope (SNOM) / scanning electron microscope hybrid system previously mentioned.
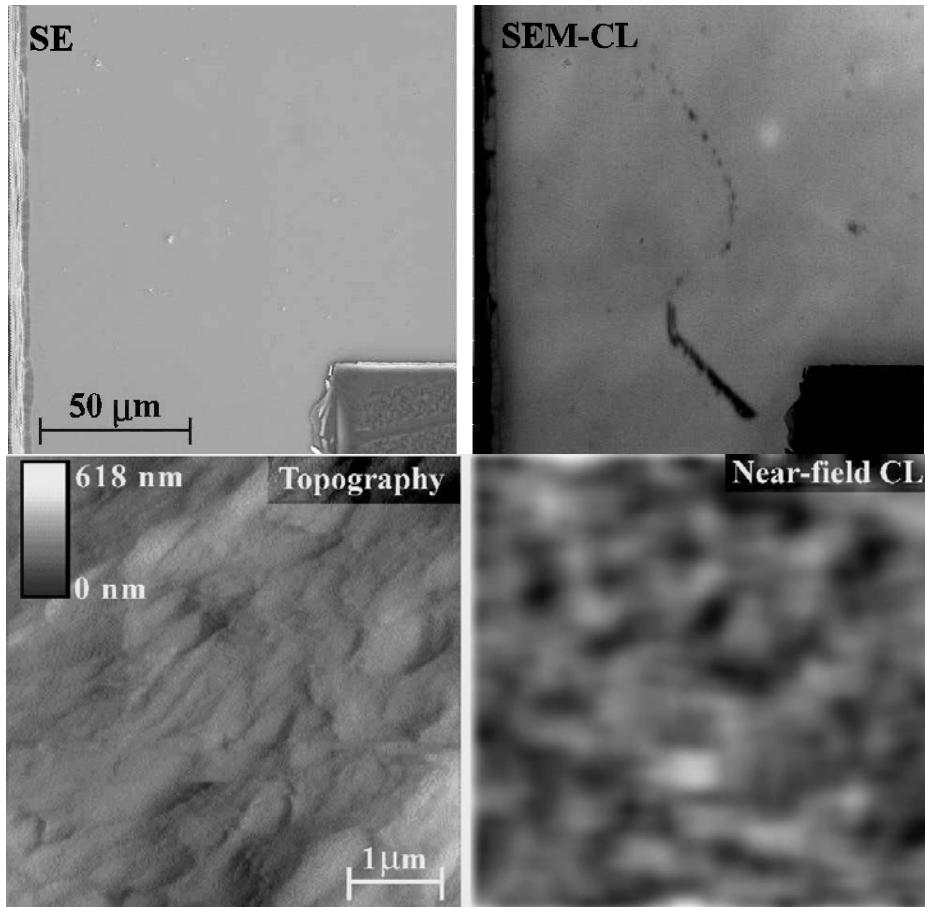
Fig. 5. Comparison between standard and near-field cathodoluminescence of LED specimen

The NF-CL results obtained at the H plasma post-treated film are illustrated in Fig 6. We investigated a grain with a diagonal of approximately 3.5 µm. From the topography image (Fig 6a) a "bubble" like structure with a height of around 100 nm is detectable. The luminescence of the so-called Band-A emission, the broad H plasma induced peak at 550 nm, and the 575 nm multi-phonon systems were separate spectrally using calibrated RGB filters (the origins of the 550 nm system and the Band-A luminescence which is located at dislocations are still not clear, because there is no theory which describes all observed phenomena). The related RGB luminescence regions, picked up directly above the recombination center and therefore independent of diffusion processes in contrast to conventional and TEM cathodoluminescence, are illustrated in Fig. 6b to Fig. 6d. Fig. 6e shows the integral NF-CL image (superimposed RGB results) The spectral dominating emission regions are depicted in Fig. 6f. White areas represent the Band-A emsission regions. H plasma induced defects and the 575 nm multi-phonon system are illustrated by gray and dark-gray areas respectively. As can be seen from these micro-graphs a lateral resolution of less than 100 nm is achievable also for these spectrally resolved measurements. A correlation of the topography and recombination centers was not found in these experiments.

Dislocations are visible clearly in the integral NF-CL image and detectable weakly only from Fig 6b and Fig. 6c. This decrease in the intensity effects therefore only the Band-A and hydrogen plasma induced luminescence but has no significant influence on nitrogen related defects. Furthermore, the Band-A and H plasma induced emission centers dominate in the vicinity of these dislocations and lead to a shift in the wavelength (blue and green) obtainable from the marked areas in Fig. 6f. A similar behavior also appears on dislocations from natural diamond that is illustrated in Fig 7. This alteration can be seen from green to blue as well as from blue to green.
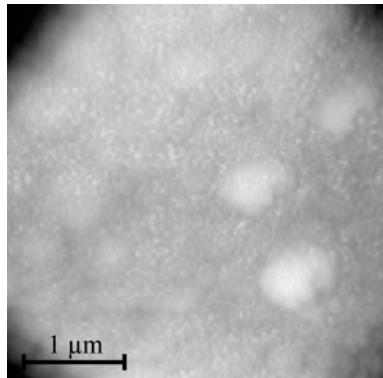
Fig. 6a: Topography of a H plasma treated diamond grain (difference in height is 600 nm).
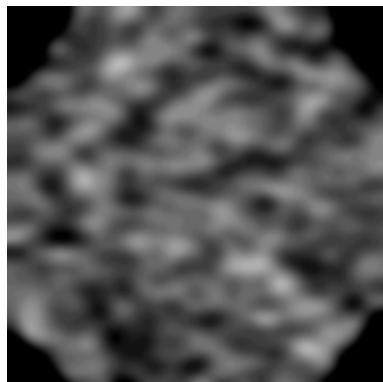

Fig. 6d: Near-field cathodoluminescence of nitrogen related efects using a calibrated red filter.

Fig. 6b: Near-field cathodoluminescence of the so-called Band-A emission using a calibrated blue filter.

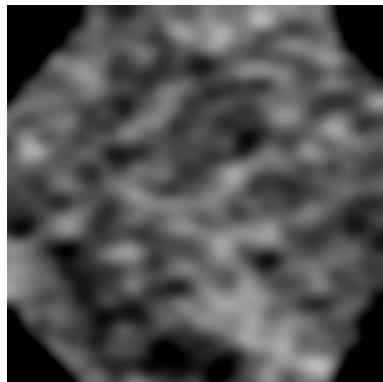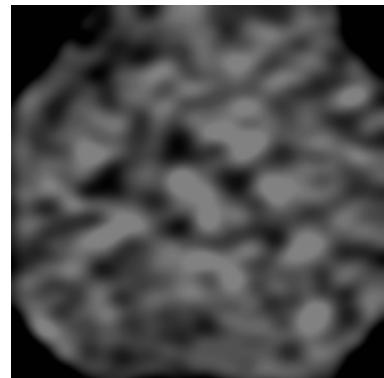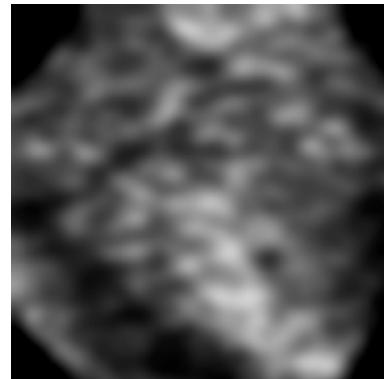Fig. 6e: Integral near-field cathodoluminescence image of the hydrogen treated diamond film.

Fig. 6c: Near-field cathodoluminescence of hydrogen plasma induced defects using a calibrated green filter.
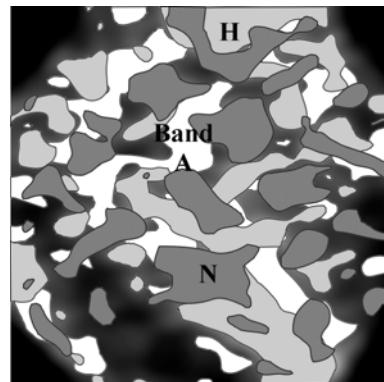

Fig. 6f: Marked areas of Fig. 3e where the Band-A, H plasma induced, and N related emission dominated.

This spectral shift was observed by time-resolved analysis for conventional CL. But this conventional analysis does not allow a local separation of defects with a high resolution due to the large diffusion length of the minorities in diamond and the fact that the generation of electron-hole-pairs and their recombination can be at different positions. From this NF-CL investigations two separated recombination centers are visible clearly now.
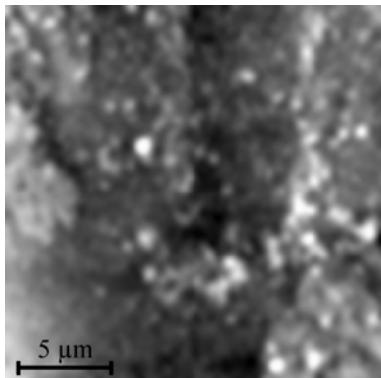
Fig.7a: Topography obtained on a natural diamond (difference in height is 150 nm).
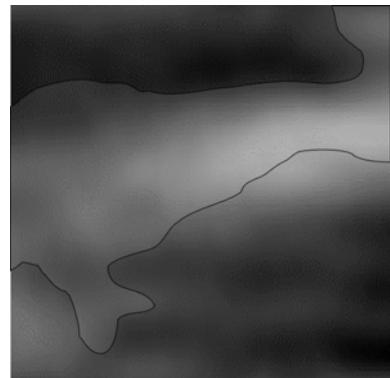

Fig. 7b: Green-blue shift obtained with NF-CL analysis of dislocations on this natural diamond grain.

Without taking into account the decrease in intensity at dislocations the Band-A and the H plasma induced luminescence regions are spread randomly over the sample surface. A cluster structure can be detected in the emission image of the 575 nm multi-phonon system (see marked areas in Fig. 6d). The luminescence of the 630 nm and 700 nm peak is negligible in this micro-graph due to the low intensity and small FWHM (number of detected phonons) of these centers. These luminescence islands have a diameter of approximately 200 nm and correlate in size and distribution with the observed "n-regions" investigated by nano electron beam induced current (nano-EBIC) characterizations. Of course, cathodoluminescence investigations cannot distinguish directly between p- and n-behavior of a semiconductor, but allow to analyze local densities of defects and their binding energies. Therefore the electronic structure detected by nano-EBIC can be explained by the coexistence of nitrogen and vacancies as presumed from panchromatic NF-CL investigations in reference.

On the other hand, the electronic behavior can be analyzed indirectly by keeping the SNOM probe at a fixed position while scanning the primary electron beam if the diffusion lengths are known. An example of the contactless determination of the local minority diffusion length by the exponential decay of the CL signal extracted from a line scan is illustrated in Fig.4. A micrograph of a used glass-fiber tip is superimposed schematically on the luminescence image.

Diffusion lengths of 1.8 µm and 1.6 µm were determined at the arbitrary positions. These values correspond to the results obtained by nano-EBIC investigations for electrons and holes respectively and are therefore an additional indicator for the presumed electric model.

Nanolithography wit Scanning Probe Microscope

Permanent decrease of design norms (i.e. of minimal size of elements) is a main tendency of modern microelectronic technology. Nowadays microelectronics provides industriall production of integrated circuits (IC) with design norm of 0.18 µm. It is based on the system of novel technologies, materials and complicated optical equipment for projection patterning. However, standard technology is not acceptable in this case due to smart price and some principal limitations that could be overridden using SPM.

The system operates in a tapping-mode and provides both high-resolution lithography and non-destructive metrology of IC components without sample vacuumization. The specimen is not subjected to any mechanical or radiative influence during the analysis and can be used in subsequent technological processes. The great advantage of the system is the ability to analyze conducting as well dielectric layers and alternations "conductor-dielectric". Different parameters can be controlled:

   linear dimensions;

   microrelief and surface topology;

   vertical structure (layer thickness, steps overlapping, channel length).

The thickness of the resist layer should not exceed required resolution. "Microposit-51813SP15" (Shipley) developed for submicron technology has been used in this work. Deposition

time of 10-50 s and rotation speed of 2000-7000 rpm were explored for finding optimal parameters. Thickness decrease was obtained by resist viscosity reduction by the solvent. In order to remove the solvent the deposited resist were dried at 102-104^{0}C. This temperature range was selected thus to avoid molecular destruction due to thermochemical processes.

Thickness and refractive index of produced films were defined by means of laser ellipsometry. All films reveal the value of refractive index 1.64. The thickness decreases from 120 to 40 nm at rotation speed increase from 5500 to 7000 rpm.

For nanolithography application the thickness of resist films must be in a range of 30-100 nm. The upper limit depends on maximal voltage V_{max} applied to probe-sample system. In this case V_{max}=100V. Since breakdown tension for thin dielectrical layers E_b= 10^9 V/m therefore maximal thickness of resist is 100 nm. The lower limit of 30 nm is conditioned by impossibility to obtain high quality of resist film at present.
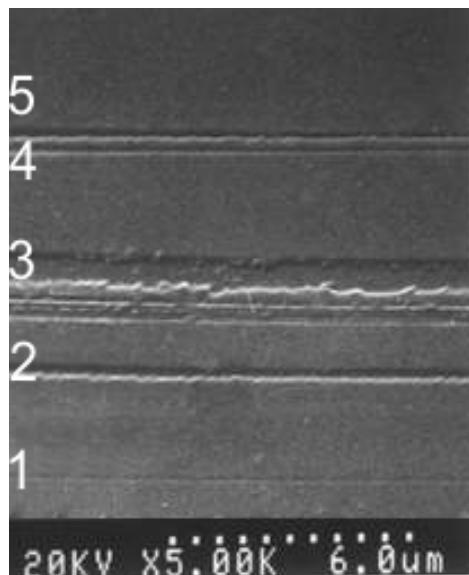

Fig. 8. SEM images of lines fabricated in resist film

There are some special requirements to defect absence in the film. Film defects were defined by etching of the hardened resist film on the Al film deposited on Si wafer. Etching was performed in a special etchant "B" (H_3PO_4 : CH_3COOH : HNO_3 : H_2O = 16 : 1 : 1 : 2 by volume) at 55^{0}C during 20 min with following calculation of etched Al points on 2x2 mm^2 square. Average number of etched points on 5 modules by perpendicular directions to base edge on 15 mm distance from the edge gives film defect quality. Average defect density is counted as average defect amount to module square ratio. The test is passed if defect density is equal to zero.

The next process of thin film resist mask fabrication has been developed:

chemical cleaning of wafers

resist preparation

resist deposition on to the wafer (~ 0.5 ml) on "Lada-125"

resist thin layer formation (5500 – 7500 rpm)

wafer placement into the dark container

resist drying in thermostat at the temperature 102-104^{0}C

resist exposition with:

100 W halogen lamp (1 min)

electrical current of 10^{-7}-10^{-9} A through the resist layer with use of scanning probe

resist development:

developer preparation: mixing of standard developer with water (9:1)

development 0.5 - 1.0 min.

development visual control

resist hardening at the temperature of 110 ^{0}C during 30 min in the thermostat

resist thickness measurements in five points: in the center of the wafer, and 1 cm from the edge by two perpendicular diameters

refractive index control

defect control

SEM topography images of fabricated submicron lines is shown in Fig.8 and the metrology results are collected in Table 1. Evidently, the following exposition regime is rather preferable: probe voltage – less than 15 V, electron current – less than 5 mA, scanning step in tapping mode – as maximal as possible. In this case the acquired lines will possess a minimal width and clear shape.

Line N	Exposition parameters			Line width, nm
	U, V	I, μA	Scanning step, μm	
1	15	5.0	14	50
2	15	6.6	1	600
3	20	8.3	1	1500
4	17	6.6	14	200
5	17	6.6	10	300

Conclusion

The presented results show only few several sides of deep and successful collaboration between BSUIR and BUW. The gain of that is not only mutual benefit of two scientific groups and closely related public. In 2001 within an individual DAAD grant Dr. R. Heiderhoff gave lectures on scanning probe microscopy analytical methods for students and researchers of BSUIR. Many researchers from other Belarusian scientific organizations took part attracted by great interest to the subject because this kind of scientific tools is still under development in Republic of Belarus. This is even more significant that at the same time BUW presented to BSUIR scanning probe microscope "AFM-Nanotec-Bermad" and scanning electron microscope "Cambridge Stereoscan" which are used in Center of Nanoelectronics and Novel Materials not only for performing research but for giving to students a deep knowledge on prospective analytical and technological methods. Both groups are not intended to stop by the achieved results. They are realizing new projects and plan further long-term cooperation.

Acknowledgment

Authors would like to thank the administrations of their Universities and all colleagues for many-sided support and help.

SCANNING PROBE MICROSCOPY
AS A COMPREHENSIVE MICROANALYTICAL INSTRUMENTARY

O.V. SERGEEV, N.V. GAPONENKO, N.G. LAZAREVA,
R.M. CRAMER, R. HEIDERHOFF, V.E. BORISENKO, L.J. BALK

Abstract

В данном обзоре кратко представлены результаты совместных работ по развитию методов микроанализа и нанолитографии на базе сканирующей зондовой микроскопии, полученные в ходе долгосрочного сотрудничества между Центром наноэлектроники и новых материалов Белорусского государственного университета информатики и радиоэлектроники (Беларусь) и кафедры электроники университета г. Вупперталь (Германия).

References

1. *Gaponenko N.V., Sergeev O.V., Misiewicz J., et al.* // Proceedings of International Conference on Solid State Crystals '98 "Epilayers and Heterostructures in Optoelectronics and Semiconductor Technology". Zakopane, Poland. 1998. P. 239-242.

2. *Cramer R.M., Sergeev O.V., Heiderhoff R., Balk L.J.* // Journal of Microscopy. 1999. Vol.194, № 2/3. P. 412-414.

3. Heiderhoff R. , Sergeev O.V., Liu Y.Y., Phang J.C.H., Balk L.J.// Journal of Crystal Growth. 2000. Vol. 201. P. 303-306.

4. *Sergeev O.V., Gaponenko N.V., Borisenko V.E., Heiderhoff R., Balk L.J.*// Proceedings of Belarusian Engineering Academy. 2000. № 1(9)/2. P.5-8.

5. *Sergeev O.V., Gaponenko N.V., Parkun V.M., et al.* // Abstracts of ASST 2000. Machester, England. 2000. P. 47.

6. *Sergeev O.V., Borisenko V.E., Heiderhoff R., Balk L.J.*// Proceedings of Scanning Probe Microscopy Workshop BelSPM-2000. Gomel , Belarus. October 24-25, 2000. P.36-40.

7. *Gaponenko N.V., Sergeev O.V., Pivin J.C., et al.* // Abstracts of MMN-2000. Athens, Greece. 2000. P. 107.

8. *Sergeev O.V., Molchan I.S., Gaponenko N.V., et al.* // Proceedings of Scanning Probe Microscopy Workshop BelSPM-2000. Gomel, Belarus. October 24-25, 2000. P. 40-44.

9. *Gaponenko N.V., Sergeev O.V., Stepanova E.A., et al.*// Journal of The Electrochemical Society. 2001. Vol.148 (2). PP. H13-H16.

10. *Sergeev O.V., Borisenko V.E., Heiderhoff R., Balk L.J.*// Physics, Chemistry and Application Of Nanostructures: Reviews and Short Notes to Nanomeeting-2001. World Scientific Publishing Co. Pte. Ltd. 2001. P.210-213.

11. *Heiderhoff R., Cramer R.M., Sergeev O.V., Balk L.J.* // Diamond and Related Materials 10: (9-10), Sep-Oct 2001. PP.1647-1651.

12. *Sergeev O.V., Chigir G.G., Emelyanov V.A. et al.* // Proceedings of Belarusian Engineering Academy. 2001. № 1(1)/2. P.15-18.